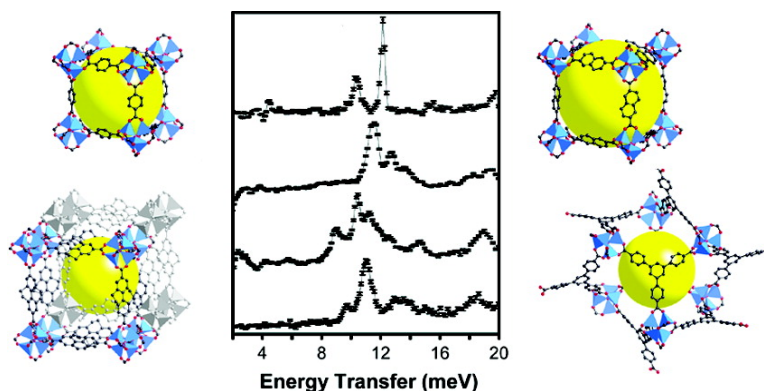


## Characterization of H Binding Sites in Prototypical Metal–Organic Frameworks by Inelastic Neutron Scattering

Jesse L. C. Rowsell, Juergen Eckert, and Omar M. Yaghi

*J. Am. Chem. Soc.*, **2005**, 127 (42), 14904-14910 • DOI: 10.1021/ja0542690 • Publication Date (Web): 30 September 2005

Downloaded from <http://pubs.acs.org> on March 25, 2009



### More About This Article

Additional resources and features associated with this article are available within the HTML version:

- Supporting Information
- Links to the 51 articles that cite this article, as of the time of this article download
- Access to high resolution figures
- Links to articles and content related to this article
- Copyright permission to reproduce figures and/or text from this article

[View the Full Text HTML](#)

## Characterization of H<sub>2</sub> Binding Sites in Prototypical Metal–Organic Frameworks by Inelastic Neutron Scattering

Jesse L. C. Rowsell,<sup>†</sup> Juergen Eckert,<sup>\*‡</sup> and Omar M. Yaghi<sup>\*†</sup>

Contribution from the Department of Chemistry, University of Michigan, 930 North University Avenue, Ann Arbor, Michigan 48109, Materials Research Laboratory, University of California, Santa Barbara, California 93106, and LANSCE-12, Mail Stop H805, Los Alamos National Laboratory, Los Alamos, New Mexico 87545

Received June 28, 2005; E-mail: juergen@mrl.ucsb.edu; oyaghi@umich.edu

**Abstract:** The hindered rotor transitions of H<sub>2</sub> adsorbed in the chemically related and prototypical porous metal–organic frameworks IRMOF-1, IRMOF-8, IRMOF-11, and MOF-177 were studied by inelastic neutron scattering to gain information on the specifics of H<sub>2</sub> binding in this class of adsorbents. Remarkably sharp and complex spectra of these materials signify a diversity of well-defined binding sites. Similarities in the spectral features as a function of H<sub>2</sub> loading and correlations with recent crystallographic studies were used to assign transitions ranging in rotational barrier from <0.04 to 0.6 kcal/mol as corresponding to localized adsorption sites on the organic and inorganic components of these frameworks. We find that binding of H<sub>2</sub> at the inorganic cluster sites is affected by the nature of the organic link and is strongest in IRMOF-11 in accord with our adsorption isotherm data. The sites on the organic link have lower binding energies, but a much greater capacity for increases in H<sub>2</sub> loading, which demonstrates their importance for hydrogen uptake by these materials.

### Introduction

The problem of hydrogen storage for mobile applications has been a critical focus in materials research over the past few decades. A wide range of solids have been examined for their ability to take up and release large amounts of molecular hydrogen to facilitate the use of hydrogen as an environmentally friendly alternative to fossil fuels.<sup>1</sup> These range from metals or alloys that dissociate H<sub>2</sub> upon adsorption and form solid solutions or compounds, to highly porous materials that physisorb molecular hydrogen within their cavities. Each class has its own merits and deficiencies, yet neither has given rise to a material that satisfies the many targeted criteria delineated by the United States Department of Energy and other national energy agencies.<sup>2</sup> Among the subset of highly porous materials, metal–organic frameworks (MOFs) have been identified only recently as potential candidates for this role.<sup>3</sup> These materials

differ greatly from classical porous materials, such as zeolites and activated carbons, primarily in their mode of construction: molecular building units are employed with predefined functionality and geometry to assemble solids, which may exhibit desired characteristics in the assembled form.<sup>4</sup> It is envisioned that once the chemical and structural aspects for enhanced hydrogen storage are elucidated, a material incorporating the essential factors can be produced in a straightforward manner.

A substantial number of potentially porous metal–organic frameworks are already known, but only a small fraction of these have been evaluated for their hydrogen uptake.<sup>5</sup> Among these, frameworks built from the linking of octahedral Zn<sub>4</sub>O(O<sub>2</sub>C–)<sub>6</sub> clusters with polyaromatic moieties have been shown to have some of the highest porosities known,<sup>6</sup> and are now of significant interest for the evaluation of their hydrogen storage

<sup>†</sup> University of Michigan.

<sup>‡</sup> University of California and Los Alamos National Laboratory.

- (1) (a) Schlappbach, L. *MRS Bull.* **2002**, *27*, 675–676 and other articles in this special issue. (b) Sandroock, G. *J. Alloys Compd.* **1999**, *293*–295, 877–888. (c) Grochala, W.; Edwards, P. P. *Chem. Rev.* **2004**, *104*, 1283–1315. (d) Schüth, F.; Bogdanovic, B.; Felderhoff, M. *Chem. Commun.* **2004**, 2249–2258. (e) Becher, M.; et al. *C. R. Phys.* **2003**, *4*, 1055.
- (2) (a) *Hydrogen Storage Materials Workshop Proceedings*; United States Department of Energy, August 14–15, 2002; [http://www.eere.energy.gov/hydrogenandfuelcells/pdfs/h2\\_stor\\_mat\\_work\\_proceedings.pdf](http://www.eere.energy.gov/hydrogenandfuelcells/pdfs/h2_stor_mat_work_proceedings.pdf). (b) *Basic Research Needs for the Hydrogen Economy*; United States Department of Energy, report of the Basic Energy Sciences Workshop on Hydrogen Production, Storage, and Use, May 13–15, 2003; <http://www.sc.doe.gov/bes/hydrogen.pdf>. (c) Tzimas, E.; Filiou, C.; Peteves, S. D.; Veyret, J.-B. *Hydrogen Storage: State-of-the-Art and Future Perspective*; European Commission DG JRC Institute for Energy, Petten 2003; [http://www.jrc.nl/publ/2003\\_publ.html](http://www.jrc.nl/publ/2003_publ.html).
- (3) Rosi, N. L.; Eckert, J.; Eddaoudi, M.; Vodak, D. T.; Kim, J.; O'Keeffe, M.; Yaghi, O. M. *Science* **2003**, *300*, 1127–1129.

- (4) (a) Rowsell, J. L. C.; Yaghi, O. M. *Microporous Mesoporous Mater.* **2004**, *73*, 3–14. (b) Kitagawa, S.; Kitaura, R.; Noro, S.-I. *Angew. Chem., Int. Ed.* **2004**, *43*, 2334–2375. (c) Janiak, C. *Dalton Trans.* **2003**, 2781–2804.
- (5) (a) Rowsell, J. L. C.; Millward, A. R.; Park, K. S.; Yaghi, O. M. *J. Am. Chem. Soc.* **2004**, *126*, 5666–5667. (b) Férey, G.; Latroche, M.; Serre, C.; Millange, F.; Loiseau, T.; Percheron-Guégan, A. *Chem. Commun.* **2003**, 2976–2977. (c) Dybtsev, D. N.; Chun, H.; Yoon, S. H.; Kim, D.; Kim, K. *J. Am. Chem. Soc.* **2004**, *126*, 32–33. (d) Pan, L.; Sander, M. B.; Huang, X.; Li, J.; Smith, M.; Bittner, E.; Bockrath, B.; Johnson, J. K. *J. Am. Chem. Soc.* **2004**, *126*, 1308–1309. (e) Kesanli, B.; Cui, Y.; Smith, M. R.; Bittner, E. W.; Bockrath, B. C.; Lin, W. *Angew. Chem., Int. Ed.* **2005**, *44*, 72–75. (f) Lee, E. Y.; Suh, M. P. *Angew. Chem., Int. Ed.* **2004**, *43*, 2798–2801. (g) Dybtsev, D. N.; Chun, H.; Kim, K. *Angew. Chem., Int. Ed.* **2004**, *43*, 5033–5036. (h) Zhao, X.; Xiao, B.; Fletcher, A. J.; Thomas, K. M.; Bradshaw, D.; Rosseinsky, M. J. *Science* **2004**, *306*, 1012–1015. (i) Chen, B.; Ockwig, N. W.; Millward, A. R.; Contreras, D. S.; Yaghi, O. M. *Angew. Chem., Int. Ed.* **2005**, *44*, 4745. (j) Lee, E. Y.; Jang, S. Y.; Suh, M. P. *J. Am. Chem. Soc.* **2005**, *127*, 6374–6381.
- (6) (a) Li, H.; Eddaoudi, M.; O'Keeffe, M.; Yaghi, O. M. *Nature* **1999**, *402*, 276–279. (b) Chae, H. K.; Siberio-Perez, D. Y.; Kim, J.; Go, Y.-B.; Eddaoudi, M.; Matzger, A. J.; O'Keeffe, M.; Yaghi, O. M. *Nature* **2004**, *427*, 523–527.

properties. These materials may also serve as models for improving our understanding of H<sub>2</sub>–adsorbent interactions because of their high degree of crystallinity, in contrast to nanostructured carbons and other disordered porous materials. Many of the most promising MOFs also exhibit highly symmetric structures, which provide simplified models for experimental and computational study. MOF-5, for example, is constructed by octahedrally linking Zn<sub>4</sub>O(O<sub>2</sub>C<sup>−</sup>)<sub>6</sub> clusters with linear phenylene links, which results in a primitive cubic framework with intersecting pseudo-spherical pores. Previous studies of this material showed that not only can adsorbates such as N<sub>2</sub> and Ar fill its evacuated pores, but H<sub>2</sub> is also adsorbed to a substantial degree.<sup>3,6</sup> More importantly, replacement of the organic link with extended and adorned aromatic units alters the hydrogen uptake in the series of compounds of which this is the prototype.<sup>5a</sup> These studies provided the first indication that simple changes in the molecular building blocks used to assemble MOFs could improve their H<sub>2</sub> storage capabilities.

Given that the structures of these compounds are well-defined, a solid foundation is provided for spectroscopic analyses of the interaction of H<sub>2</sub> with the framework atoms. Such studies provide crucial details for the interpretation of bulk adsorption measurements such as the structural features that may be responsible for enhanced hydrogen uptake. The method that is most sensitive to the chemical environment of adsorbed H<sub>2</sub> is inelastic neutron scattering (INS) spectroscopy of the hindered rotational transitions of the adsorbed molecules. The success of this technique for the present application stems from the uniquely large neutron scattering cross-section of <sup>1</sup>H and the fact that neutrons can be used to observe transitions in the hydrogen molecule that involve a change in the total nuclear spin of the molecule. This is important because rotational transitions with a change in the molecular rotational quantum number  $\Delta J = \text{odd}$  are forbidden for H<sub>2</sub> in optical spectroscopy because this transition is coupled with a change in the nuclear spin wave function  $\Delta I = \pm 1$ . The reason for this is that the overall molecular wave function has to be antisymmetric with respect to the rotational exchange of the identical fermions.<sup>7</sup> Thus, *para*-H<sub>2</sub> (antiparallel <sup>1</sup>H spins) is only associated with even/symmetric *J* states, while *ortho*-H<sub>2</sub> (parallel <sup>1</sup>H spins) must have odd/antisymmetric *J* states. The lowest rotational transition (*ortho* → *para* H<sub>2</sub> for the free rotor) occurs at 14.7 meV and decreases rapidly with the application of a potential barrier to rotation. Such potentials are encountered when H<sub>2</sub> is in a bound state, such as in  $\sigma$ -complexes<sup>8</sup> or when physisorbed on a surface. Consequently, the use of INS has made it possible to determine fine details of hydrogen adsorption in a wide variety of materials including zeolites,<sup>9</sup> nanoporous nickel phosphate VSB-5,<sup>10</sup> C<sub>60</sub>,<sup>11</sup> and carbon nanostructures.<sup>12</sup>

In our first report of hydrogen storage by MOFs, we observed exceptionally well-defined multiple binding sites for hydrogen within the cavities of MOF-5 (=IRMOF-1) by INS with some of these being associated with the organic linking group. We now expand these studies to other promising MOFs constructed from Zn<sub>4</sub>O(O<sub>2</sub>C<sup>−</sup>)<sub>6</sub> units, including IRMOF-8, IRMOF-11, and MOF-177, to investigate to role of the organic linking group on hydrogen binding. We find that the nature of the distinct H<sub>2</sub>

binding within the pores varies considerably among the four materials despite the apparent simplicity of this family of structures, and thereby gives clear indication that the organic linking units play a significant role in the adsorption of hydrogen.

## Experimental Section

**Sample Preparation.** The porous MOFs were synthesized by the solvothermal reaction of Zn<sup>2+</sup> with the corresponding linking carboxylates, followed by exchange of the included solvent molecules by immersion in chloroform, and evacuation at room temperature as described previously.<sup>5a</sup> The crystalline phase purity of each sample was confirmed by comparing the powder X-ray diffraction patterns (Bruker-AXS D8 Advance diffractometer in Bragg–Brentano geometry using Cu K $\alpha$  radiation) with those calculated from single crystal data. The sample porosities were found to be comparable to the values previously reported for these materials by gravimetric determination of the N<sub>2</sub> and H<sub>2</sub> capacities at 77 K in the 0–1 atm range.<sup>5a</sup>

**Inelastic Neutron Scattering.** The evacuated MOF samples were transferred under helium to a cylindrical aluminum sample cell (10 cm<sup>3</sup> capacity) sealed with an indium gasket and connected to an external gas manifold by a stainless steel capillary. The cell was mounted in a closed-cycle helium refrigerator. After thorough evacuation of the sample cell at room temperature, the INS spectrum of the “blank” sample was collected at 15 K followed by data acquisition with various loadings of H<sub>2</sub>. We note that the spectra of the host materials were identical after desorption of hydrogen to those collected initially, which confirms the fully reversible nature of hydrogen adsorption in MOFs. Gas loading was carried out in situ with the sample cell at 60–100 K by monitoring the pressure drop from the calibrated volume of the manifold. Inelastic neutron scattering spectra were acquired on the QENS spectrometer at the Intense Pulsed Neutron Source at Argonne National Laboratory. QENS is an inverse geometry time-of-flight instrument in which a pulsed “white” beam is incident on the sample. Only those neutrons with energies low enough (3.6 meV) to fall within a small band determined by diffraction from an array of graphite analyzers reach the detectors. The incident neutron energy is scanned by time-of-flight, and INS spectra collected on QENS correspond mainly to neutron energy loss. Standard data reduction programs were used for normalization of the data and conversion to a linear energy scale.

**Spectral Analysis.** As all of the evacuated MOFs in this study exhibit some bands at low frequency, whose origin is unclear at this point, our assignments of the spectra of H<sub>2</sub> loaded samples were aided by subtraction of the spectrum collected from the “blank”. Assignment of the peaks in the INS spectra was performed with the use of a single-parameter model for the rotational potential. This model uses the energy eigenvalues for the H<sub>2</sub> rotations with two angular degrees of freedom in a double-minimum potential, as described previously.<sup>9b</sup> The rotational energy levels of the free hydrogen molecule are given by  $BJ(J + 1)$ , where *B* is the rotational constant (taken to be 7.35 meV) and *J* is the rotational quantum number. Application of a barrier to rotation removes some of the degeneracy of the *J* levels and drastically changes the level

(7) Silvera, I. F. *Rev. Mod. Phys.* **1980**, *52*, 393–452.

(8) Eckert, J.; Kubas, G. J. *J. Phys. Chem.* **1993**, *97*, 2378–2384.

(9) (a) Braid, I. J.; Howard, J.; Nicol, J. M.; Tomkinson, J. *Zeolites* **1987**, *7*, 214–218. (b) Nicol, J. M.; Eckert, J.; Howard, J. *J. Phys. Chem.* **1988**, *92*, 7117–7121. (c) Eckert, J.; Nicol, J. M.; Howard, J.; Trouw, F. R. *J. Phys. Chem.* **1996**, *100*, 10646–10651. (d) MacKinnon, J. A.; Eckert, J.; Coker, D. A.; Bug, A. L. R. *J. Chem. Phys.* **2001**, *114*, 10137–10150. (e) Mojet, B. L.; Eckert, J.; van Santen, R. A.; Albinati, A.; Lechner, R. E. *J. Am. Chem. Soc.* **2001**, *123*, 8147–8148.

(10) Forster, P. M.; Eckert, J.; Chang, J.-S.; Park, S. E.; Férey, G.; Cheetham, A. K. *J. Am. Chem. Soc.* **2003**, *125*, 1309–1312.

(11) Fitzgerald, S. A.; Yildirim, T.; Santodonato, L. J.; Neumann, D. A.; Copley, J. R. D.; Rush, J. J.; Trouw, F. *Phys. Rev. B* **1999**, *60*, 6439–6451.

(12) (a) Brown, C. M.; Yildirim, T.; Neumann, D. A.; Heben, M. J.; Gennett, T.; Dillon, A. C.; Alleman, J. L.; Fischer, J. E. *Chem. Phys. Lett.* **2000**, *329*, 311–316. (b) Ren, Y.; Price, D. L. *Appl. Phys. Lett.* **2001**, *79*, 3684–3686. (c) Schimmel, H. G.; Kearley, G. J.; Nijkamp, M. G.; Visser, C. T.; de Jong, K. P.; Mulder, F. M. *Chem.-Eur. J.* **2003**, *9*, 4764–4770.

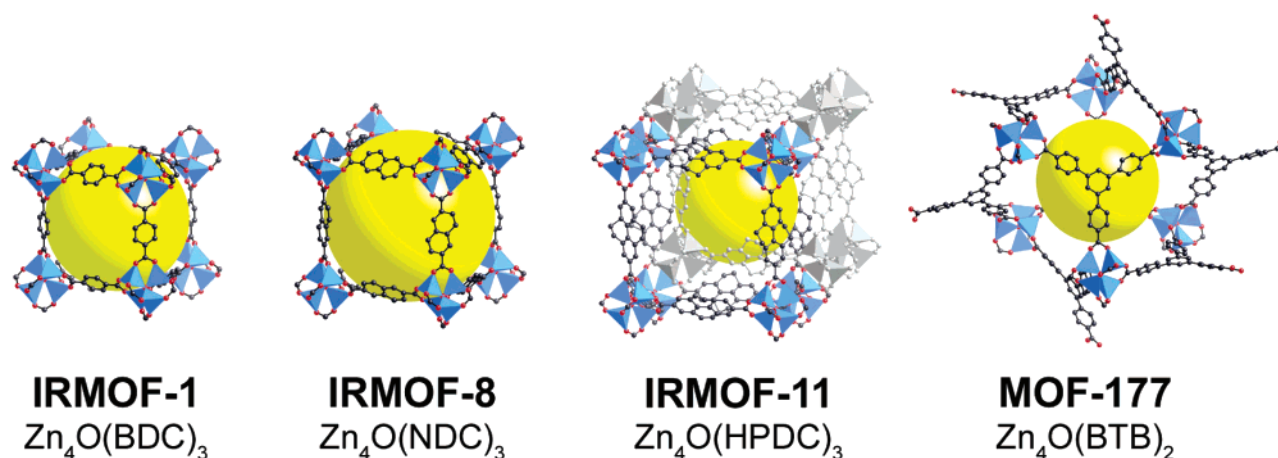


**Figure 1.** Metal–organic frameworks analyzed in this study. Topologically, the isorecticular MOFs (“IRMOFs”) are based upon an augmented simple cubic net (the boron net in  $\text{CaB}_6$ ), while MOF-177 is based upon the augmented form of the (3,6)-coordinated net **qom**. IRMOF-11 is composed of two interwoven frameworks, one shown in gray-scale. The large pore of each structure is represented by a yellow sphere with diameter defined by the distance between the van der Waals surfaces of the framework atoms. Atom colors: C black, O red, Zn blue tetrahedra, H omitted.

spacings (see Figure 4 in ref 9b). The spacing between the two lowest energy levels in fact has an approximately exponential dependence on the barrier height, which is the origin of the sensitivity of this technique to differences in the guest–host interactions of the adsorbed  $\text{H}_2$ . We label transitions for the hindered  $\text{H}_2$  rotor (e.g., 0–1) as being between energy levels that are numbered 0, 1, 2... with increasing energy. These numbers are not to be taken as the rotational quantum number  $J$ , which is only appropriate for the free rotor. Despite the low temperature of our experiments, transitions such as 1–2 may also be observable in neutron energy loss if spin conversion (i.e., *ortho*→*para* transition) for the adsorbed hydrogen molecule is as slow as in the solid or liquid. Unfortunately, our previous studies on hydrogen in zeolites and MOFs have not provided a consistent picture of this phenomenon. Spin conversion was usually found to be insignificant on the time scale of the experiment, but in a few cases sufficiently rapid to prevent observation of transitions from level 1. Our assignments, therefore, are complicated in cases where we may not have sufficient intensity for the 1–2 to make a definitive conclusion. Finally, we note that a rotational potential with separate barriers for in-plane and out-of-plane reorientation would be more realistic, as we found in our theoretical study of  $\text{H}_2$  in zeolite A;<sup>9d</sup> however, application of such a model to spectra from  $\text{H}_2$  adsorbed on multiple sites would make assignments even more difficult as at least two transitions must be reliably attributed to each site to determine the two parameters of this model.

## Results and Discussion

The materials studied here are members of a group of metal–organic frameworks constructed by linking octahedral  $\text{Zn}_4\text{O}(\text{O}_2\text{C}-)_6$  secondary building units with polyaromatic moieties. Included are IRMOF-1 constructed with benzene-1,4-dicarboxylate (BDC), IRMOF-8 from naphthalene-2,6-dicarboxylate (NDC), IRMOF-11 from 4,5,9,10-tetrahydropyrene-2,7-dicarboxylate (HPDC), and MOF-177 from fully deprotonated 1,3,5-tris(4-carboxyphenyl)benzene (=“benzene-1,3,5-tribenzoate”, BTB), as shown in Figure 1.<sup>5a</sup> The rigidity of both the clusters and the links prevents the frameworks from collapsing upon evacuation of the included guest molecules. In addition, the frameworks possess long-range order that is maintained in the absence or presence of guest molecules, which has facilitated the atomic-scale resolution of their structures from X-ray crystallographic analyses.

Although the materials studied here are chemically very similar, their capacities for hydrogen adsorption are rather

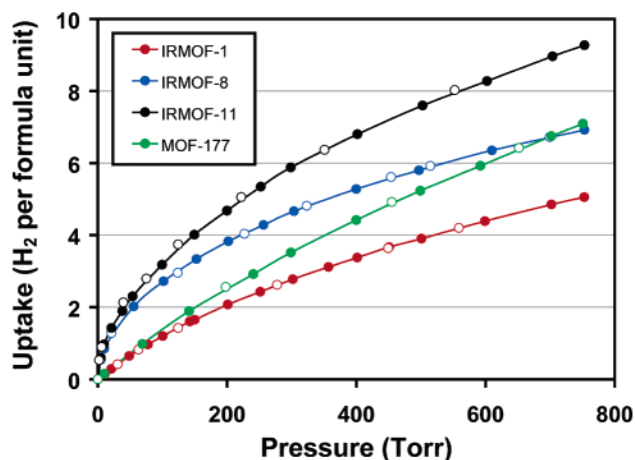


**Figure 2.** Hydrogen adsorption isotherms measured at 77 K for the MOFs analyzed in this study. Adsorption points are shown as filled circles, while desorption points are shown as open circles; data from ref 5a.

different. This is apparent when the adsorption isotherms are normalized per formula unit, as shown in Figure 2. It is clear that the organic links play important roles in defining pore sizes and providing organic adsorptive sites, but they may also alter the interaction of  $\text{H}_2$  with the cluster due to differences in their electronic structures. This is demonstrated by comparing the INS spectrum of each material at a loading of 4  $\text{H}_2$  molecules per  $\text{Zn}_4\text{O}L_x$  formula unit (Figure 3). These spectra differ markedly among the four different materials, and in all cases are exceedingly well-defined when compared with similar data for hydrogen on carbons or in zeolites,<sup>9,12</sup> providing an excellent opportunity to examine the subtle chemical differences between the pores of each material. This is facilitated by the fact that the transitions of the hindered  $\text{H}_2$  rotor observed by INS are very sensitive to the height of the barrier to rotation, which in turn depends on the chemical environment of the adsorbed molecules. The spectra in Figure 3, therefore, clearly show that adsorption sites in each material are different, despite the fact that these materials are composed of similar chemical moieties.

A feature that is common to all of the materials at this loading is the presence of at least two peaks in the INS spectra that can be assigned to transitions associated with different binding sites. This observation was made in the initial work on IRMOF-1

**Table 1.** Proposed Peak Assignments for INS Spectra Acquired from MOFs in This Study<sup>a</sup>

material	site	transition energy (meV)			potential barrier <sup>b</sup> (kcal mol <sup>-1</sup> )	comment
		0–1	0–2	1–2		
IRMOF-1	I	10.3	17.5	7.5	0.42	
	II	12.1	15.5	4.4	0.24	
	III	12.5	15.8	3.5 <sup>c</sup>	0.19	overlapping with site II
	IV	13.3	15.4	2.1 <sup>c</sup>	0.13	
IRMOF-8	I	10.8	17.2 <sup>c</sup>	6.4 <sup>c</sup>	0.36	shoulder of site II 0–1
	II	11.5	16.6	5.1 <sup>c</sup>	0.29	broad 0–2
	III	12.8	15.7	3	0.17	
	IV'	14.4	14.9	0.5 <sup>c</sup>	0.03	contains 13.7 meV peak, site IV
	Zn <sup>2+</sup> defect	8.1	19.7 <sup>c</sup>	11.6 <sup>c</sup>	0.66	weak, broad
IRMOF-11	I	8.9	18.9	10	0.56	broad 0–2
	II	10.5	17.4	7 <sup>c</sup>	0.39	0–2 overlapping with site III 0–2
	III	11.2	16.9	5.7	0.32	0–1 shifts to 11.5 meV
	IV	13.8	15.2	1.4 <sup>c</sup>	0.08	broad
MOF-177	I	9.7	18.1	8.4 <sup>c</sup>	0.47	
	II	11.1	16.9 <sup>c</sup>	5.8 <sup>c</sup>	0.33	
	III	11.7	15.6	4	0.27	0–1, 0–2 shift to higher energy
	IV	14	1 <sup>c</sup>	15.1	0.07	0–2 overlapping with site III 1–2

<sup>a</sup> Note that the peak positions calculated from the model used may not correspond exactly with observed features because of the approximation involved in the choice of model (see text). <sup>b</sup> Calculated from the model described in ref 9b. <sup>c</sup> Expected but weak or not observed. In the case of (1–2) transitions, this may be due to low population of *ortho*-H<sub>2</sub>.

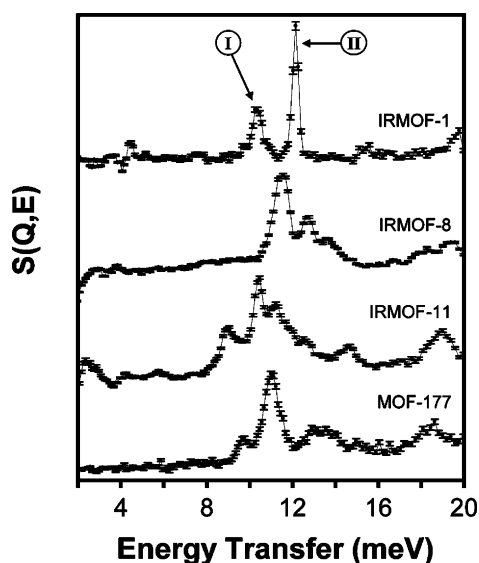


**Figure 3.** Inelastic neutron scattering spectra for each material loaded with 4 H<sub>2</sub> per formula unit. The two 0–1 transitions originally assigned to sites I and II in IRMOF-1 are labeled. Spectra are vertically offset for comparison purposes; the error bars shown are representative of all spectra.

and indicates that multiple site occupancy is occurring. Figure 1 shows that each Zn<sub>4</sub>OL<sub>x</sub> formula unit describes a complete Zn<sub>4</sub>O(O<sub>2</sub>C–)<sub>6</sub> secondary building unit, which is a cluster with octahedral shape but tetrahedral symmetry, having two inequivalent sets of four faces (although strictly speaking, the crystallographic symmetries are lower for the clusters in IRMOF-11 and MOF-177). As proposed previously, the strongest binding site should be on one of these faces, each being able to accommodate 4 H<sub>2</sub> molecules per Zn<sub>4</sub>OL<sub>x</sub> formula unit. The fact that we observe multiple peaks in each spectrum at low loading suggests that the binding energies for the different sites are not substantially different.

In assigning the spectra collected in this study, it is important to recall the hypotheses proposed in the initial work on IRMOF-1.<sup>3</sup> Adsorbed hydrogen molecules in IRMOF-1 produce spectra with the fewest and sharpest peaks, because of the extraordinary

degree of order and simplicity of its high symmetry structure. We argued previously that a site (subsequently referred to as site I) in the corner of the pore, on the inorganic cluster, ought to be the preferred binding site for H<sub>2</sub> and results in the highest barrier to rotation. The peak at 10.3 meV in the IRMOF-1 spectrum of Figure 3 was therefore assigned as the 0–1 transition for H<sub>2</sub> adsorbed on site I. The corresponding 1–2 and 0–2 transitions would then be expected at 7.2 and 17.5 meV, respectively, but there is only weak evidence for these. These assignments were verified by comparison with the INS spectrum of 4 D<sub>2</sub> molecules per formula unit and scaling the rotational energy level diagram by the respective rotational constants of H<sub>2</sub> and D<sub>2</sub>. The rotational barrier associated with site I was found to be 0.42 kcal/mol. The strong peak at 12.1 meV would then be assigned to a second binding site (labeled site II), for which the 1–2 and 0–2 transitions at 4.4 and 15.5 meV do show some weak intensity. An increase in loading to 8 molecules per formula unit resulted in increases in intensity for all three bands associated with site II as well as a new band at 12.5 meV, distinct from the main peak at 12.1 meV, accompanied by similar structure in the band near 15.4 meV. At higher loadings, other overlapping bands appear in the region of 11.5–13.5 meV, indicating that multiple sites with similar rotational barriers are occupied. Spectral assignments for all materials are summarized in Table 1.

Inspection of the loading dependence of the INS spectra of the other materials leads to similar assignments. For hydrogen in MOF-177, we observe spectral features (Figure 4) comparable to those of IRMOF-1, but with greater complexity, as would be expected from the lower symmetry and larger link of this structure. Transitions at low loading are shifted to lower energies than those in IRMOF-1, which indicates that the barriers to rotation in MOF-177 are higher. While the primary binding site at a loading of 4 molecules per formula unit is indicated by a strong 0–1 transition at 11.1 meV, a second, evidently much less populated, site has this transition at 9.7 meV. An increase in loading to 8 H<sub>2</sub> molecules per formula unit gives rise to a new band at 11.7 meV. It is accompanied by increases in the band at 15.6 meV (the 0–2 transition for this site) and a broad

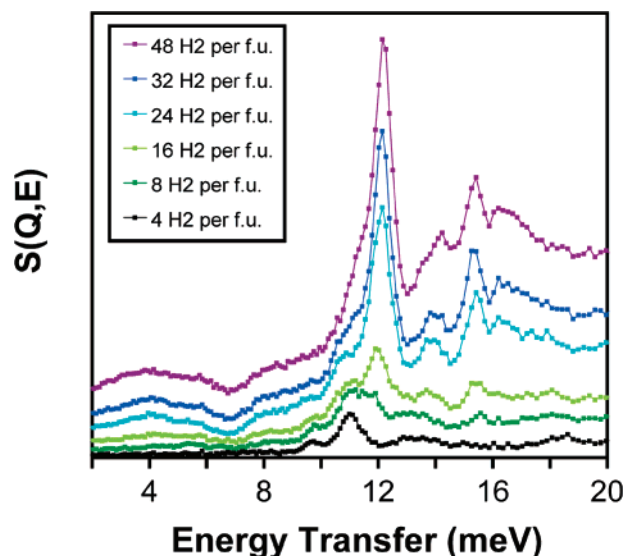


**Figure 4.** Inelastic neutron scattering spectra for MOF-177 at various loadings of  $\text{H}_2$ .

band near 4 meV (the corresponding 1–2 transition). This peak at 11.7 meV, along with the corresponding 0–2 transition, continues to gain intensity and shifts toward 12.1 meV up to the maximum loading used in our experiment, 48  $\text{H}_2$  per formula unit (=8.4 wt %). This peak is similar to the dominant peak(s) in the IRMOF-1 spectra assigned to site II. This supports the original hypothesis that site II exists on or near the organic link, as the BDC and BTB links are similar, each composed of nonfused aromatic rings, and should have similar interactions with  $\text{H}_2$ . The greater size and complexity of the BTB link, however, would give rise to more nonequivalent sites, and hence more peaks in the MOF-177 spectra, as is observed. There are at least three overlapping peaks in this region.

It should be noted at this stage that small apparent shifts in peaks, or the appearance of new intense peaks that overlap others as the loading is increased, may be interpreted in two ways: (1) increased population of new sites that are similar in rotational barrier, and perhaps chemical environment, or (2) perturbation of the chemical environment of already populated sites by interaction with  $\text{H}_2$  filling neighboring sites. With this in mind, the MOF-177 spectra may be interpreted such that at low loading we observe partial occupation of two distinct sites, at least one of which is on the inorganic cluster, followed by progressive filling of sites around the organic link. There is only enough volume surrounding the inorganic cluster to place as many as 16  $\text{H}_2$  molecules per formula unit (this is described in greater detail below), so that the prominence of the peaks around 12 meV at this loading and above indicates that they correspond to sites around the organic link. The additional appearance of intensity around 14 meV (with a small rotational barrier of 0.07 kcal/mol) at 16  $\text{H}_2$  per formula unit should, therefore, also be due to molecules adsorbed on the organic unit. There also appears to be at least two peaks in this region. This corresponds well with the very low rotational barrier that was reported for  $\text{H}_2$  on the surface of graphite<sup>13</sup> and other carbon nanostructures.<sup>12</sup> The larger barrier observed for the 12 meV peaks further implies that as sites on the organic link, they are significantly altered by connection to the inorganic cluster.

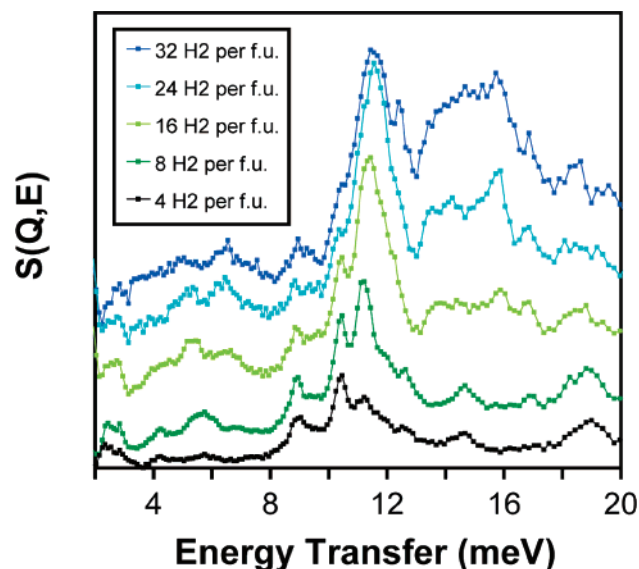


**Figure 5.** Inelastic neutron scattering spectra for IRMOF-11 at various loadings of  $\text{H}_2$ .

The spectra for IRMOF-11 are also rich in complexity, as shown in Figure 5, with well-defined peaks at low loadings that become overlapped with others as the amount of hydrogen is increased. Most notable is the observation of a peak at 8.9 meV at low loading, which is assigned to the 0–1 transition of a site with the highest barrier to rotation (0.56 kcal/mol) observed thus far in this class of materials. A comparison of the relative positions and intensities of the peaks in the spectra for 4  $\text{H}_2$  per formula unit in IRMOF-1 and IRMOF-11 (see Figure 3) leads to the assignment of the 8.9 meV peak as corresponding to site I in IRMOF-11. The equivalent peak for site II in IRMOF-11 at 10.5 meV is also shifted to lower energy as compared to IRMOF-1. These tendencies suggest that binding in IRMOF-11 is stronger than in IRMOF-1, which in turn is in qualitative accord with adsorption isotherms recently reported for these two materials, which showed a stronger uptake of  $\text{H}_2$  by IRMOF-11 as compared to IRMOF-1 (see Figure 2).

At the lowest loading, there is also clear evidence of occupation of at least one additional site in IRMOF-11 indicated by a peak at 11.2 meV. As the amount of hydrogen is increased, this peak shows behavior similar to that of the 11.7 meV peak in the spectra of MOF-177; it either shifts toward 11.5 meV or is engulfed by more intense peaks at this energy until this closely overlapping group dominates the spectrum at 32  $\text{H}_2$  per formula unit (compare Figures 4 and 5). Increased intensity is also observed in the broad regions around 5 and 14 meV, which are almost certainly composed of several unresolvable peaks. This can be attributed to the larger size of the HPDC link employed in IRMOF-11, which should accommodate more binding sites that are similar in rotational barrier. The general shifting of these peaks to lower energy highlights the importance of the link in hydrogen binding. In this case, however, it is not obvious whether these spectral shifts and the enhanced  $\text{H}_2$  uptake at 77 K are due to direct interaction with the larger organic link, or increased attractive potential due to the comparatively smaller pores in this interwoven structure.

The spectral features for hydrogen in IRMOF-8 at low loadings appear to differ markedly from those of the other materials. We considered a number of explanations for the

(13) Freimuth, H.; Wiechert, H.; Lauter, H. *J. Surf. Sci.* **1987**, *189*, 548–556.

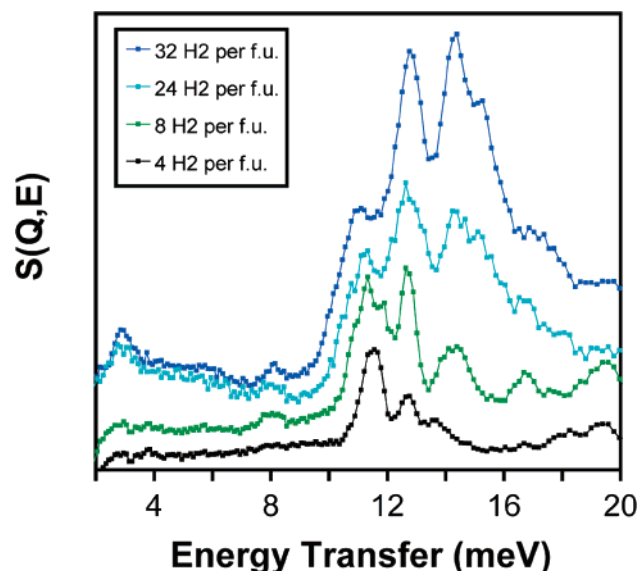


**Figure 6.** Inelastic neutron scattering spectra for IRMOF-8 at various loadings of H<sub>2</sub>.

spectrum at 4 H<sub>2</sub> per formula unit, but two seemed most probable based on comparisons to the data collected from the other materials. In the first case, the peaks corresponding to sites I and II in the IRMOF-1 spectra (see Figure 3) are similarly shifted to higher energies (11.5 and 12.8 meV), and in contrast to the IRMOF-1 spectra, “site I” at 11.5 meV has the higher occupancy in IRMOF-8 and gives rise to the more intense peak. A second possibility is that “sites I and II” in IRMOF-8 have very similar rotational barriers and their 0–1 transitions are both contained in the relatively broad band at 11.5 meV. The peak at 12.8 meV would then be attributed to a third site that is also occupied at the lowest loading, and it is this site that shows a loading dependence similar to that of the other materials. Support for the second interpretation may be provided by the presence of a small shoulder at 10.8 meV at a loading of 4 H<sub>2</sub> per formula unit, and the fact that this broad band at 11.5 meV develops noticeable structure when the loading is increased to 8 H<sub>2</sub> per formula unit.

At higher loadings, the spectral features observed for hydrogen in IRMOF-8 reveal some similarities to the other materials. As the amount of hydrogen is increased, the peak at 12.8 meV increases in intensity similar in behavior to the 11.7 meV peak in MOF-177 and the 11.2 meV peak in IRMOF-11 (see Figure 6). We therefore assign this peak to a 0–1 transition for a site around the link, with a notably smaller rotational barrier (0.17 kcal/mol; 1–2 transition appearing at 3 meV, 0–2 appearing at 15.7 meV). A broad feature also develops at 14.4 meV, with asymmetry that also implies it is composed of several overlapping peaks, which we attribute to weakly interacting sites on the link similar to those discussed above for IRMOF-11, having very small barriers to rotation of  $\sim 0.03$  kcal/mol. This is consistent with the higher carbon content of these wider links, and the observation of small rotational barriers on carbonaceous materials.<sup>11–13</sup> A sharper feature in this region appears at the highest loading, 32 H<sub>2</sub> per formula unit (=7.0 wt %), which may be due to the formation of solid hydrogen or a second layer in the pore. In addition, there is a weak and broad peak that appears at 8.1 meV that does not correspond to a 1–2 transition for the other features. As the relative intensity is small and does

not change with loading, it is unclear what binding sites in the structure it corresponds to, perhaps defects such as extraframework Zn<sup>2+</sup> cations.<sup>9a</sup>

In assigning the spectra of hydrogen adsorbed in these materials, summarized in Table 1, we have borne in mind the chemical similarities between them and hypothesized that adsorption may be strongest at sites on the inorganic cluster, which become filled with loading followed by population of sites around the organic links. This hypothesis is supported by other studies recently reported in the literature, including computations of H<sub>2</sub> in IRMOF-1<sup>14</sup> and low-temperature single-crystal diffraction analyses of argon and dinitrogen adsorbed in this material.<sup>15</sup> In the computational report, second-order Møller–Plesset perturbation theory was used to compare the binding energies of H<sub>2</sub> to organic and inorganic fragments of the IRMOF-1 structure. In combination with adsorbate density analysis using Monte Carlo simulations of H<sub>2</sub> in a unit cell of IRMOF-1, it was concluded that at low temperatures the strongest binding sites were found in the corners of the large pores, on faces of the Zn<sub>4</sub>O(O<sub>2</sub>C–)<sub>6</sub> clusters.

Our conclusions on the identities of the adsorption sites for hydrogen have been corroborated experimentally by Rowsell et al. in variable-temperature X-ray diffraction studies of argon and dinitrogen adsorbed in single crystals of IRMOF-1.<sup>15</sup> The remarkable localization of electron density attributable to adsorbed atoms in this structure was attained experimentally at temperatures as low as 30 K using novel low-temperature X-ray instrumentation.<sup>16</sup> We briefly recall the results obtained in ref 15 to provide further details on the likely binding sites for hydrogen in these MOFs. Although direct comparison of these results on Ar and N<sub>2</sub> with the behavior of H<sub>2</sub> adsorbed in the pores may not be rigorous, the structural details obtained in that study have granted us additional insight in the interpretation of the INS spectra. The principal binding site for N<sub>2</sub> and Ar in IRMOF-1 is at a position equidistant from three carboxylates, on one of the two independent faces of the octahedral inorganic cluster. This site, denoted  $\alpha(\text{CO}_2)_3$  and illustrated in Figure 7, showed the maximum extraframework electron density calculated from diffraction data collected from IRMOF-1 in the presence of N<sub>2</sub> or Ar. Despite the weaker van der Waals interaction of H<sub>2</sub> with the IRMOF-1 surface, we hypothesize that this position is also the principal binding site for H<sub>2</sub> and gives rise to the 0–1 transition at 10.3 meV in the INS spectra of IRMOF-1 (see Figure 3). There are four of these sites per formula unit, and so the observation of an additional peak at 12.1 meV at this loading indicates that only a small difference in binding energy exists between this and a neighboring site. During cooling, multiple sites are sampled by H<sub>2</sub> diffusing on the surface until the point at which their motion is frozen out, not necessarily at the global minimum in energy. This observation has been made previously in extensive studies of H<sub>2</sub> adsorbed in zeolites.<sup>9</sup>

A total of five primary binding sites were identified for gases in IRMOF-1, including three on the inorganic cluster and two solely on the phenylene link.<sup>15</sup> These are shown schematically in Figure 7. By refining the adsorbate site occupancies as a function of temperature, the relative binding energies were

(14) Sagara, T.; Klassen, J.; Ganz, E. *J. Chem. Phys.* **2004**, *121*, 12543–12547.

(15) Rowsell, J. L. C.; Spencer, E. C.; Eckert, J.; Howard, J. A. K.; Yaghi, O. M. *Science* **2005**, *309*, 1350.

(16) Goeta, A. E.; Howard, J. A. K. *Chem. Soc. Rev.* **2004**, *33*, 490.

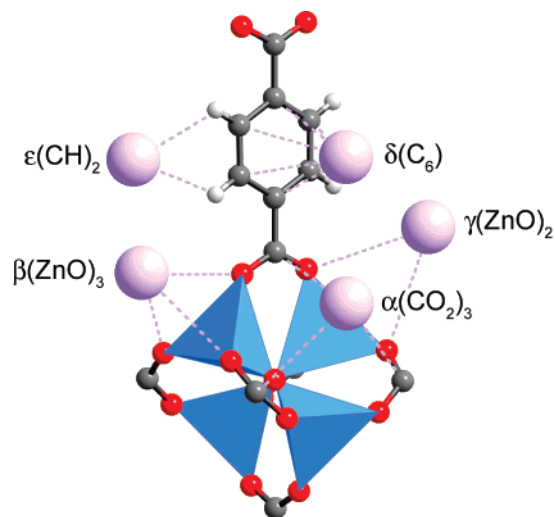


**Figure 7.** Proposed binding sites for  $\text{H}_2$  in IRMOF-1 and related frameworks in accordance with the electron density attributable to adsorbed argon (purple spheres) detected by X-ray diffraction analysis at 30 K.<sup>15</sup> These are  $\alpha(\text{CO}_2)_3$  above one face of the octahedral inorganic cluster, equidistant to three carboxylates,  $\beta(\text{ZnO})_3$  above the face of a  $\text{ZnO}_4$  tetrahedron,  $\gamma(\text{ZnO})_2$  above the edge of a  $\text{ZnO}_4$  tetrahedron,  $\delta(\text{C}_6)$  on the  $\text{C}_6\text{H}_4$  phenylene face, and  $\epsilon(\text{CH})_2$  on the phenylene edge. Atom colors: C black, H white, O red, Zn blue tetrahedra.

concluded to be in the order  $\alpha(\text{CO}_2)_3 \gg \beta(\text{ZnO})_3 > \gamma(\text{ZnO})_2 > \delta(\text{C}_6) \approx \epsilon(\text{CH})_2$ . It was found, however, that the occupation of the  $\gamma(\text{ZnO})_2$  site was preferred over  $\beta(\text{ZnO})_3$  at lower temperatures, most likely due to the greater multiplicity of that site and the resultant increase in packing efficiency on the cluster surface. Each  $\alpha(\text{CO}_2)_3$  site is surrounded trigonally by  $\gamma(\text{ZnO})_2$  sites at 4 Å, and so each cluster can accommodate at most 16 adsorbed molecules per formula unit. In the INS spectra, we therefore expect two unique 0–1 transitions for these sites, in a 1:3 intensity ratio, saturating at approximately 16  $\text{H}_2$  per formula unit. Aside from variance in peak positions, and possible overlap in the case of IRMOF-8, this is what is observed in this study, and we conclude that sites I and II are  $\alpha(\text{CO}_2)_3$  and  $\gamma(\text{ZnO})_2$ . At higher loadings, we expect the faces and edges of the organic links to become occupied, and this is signified in a more narrow spectral range by the appearance of new peaks, specifically, one strong peak around 12 meV and several overlapping peaks in the range 11–16 meV (including 0–2 transitions), which are characteristic of the link. In the case of IRMOF-1, and perhaps IRMOF-8, this appears to coincide with site II giving the impression of fewer sites, or greater equivalence of neighboring sites. As noted above, exact correspondence between the INS spectral intensities and the expected site occupancies is rarely observed because of the low energy barrier

between neighboring sites and the tendency for  $\text{H}_2$  to be stranded on adjacent sites after their diffusion is thermally quenched.

### Summary

We have obtained remarkably detailed information on the primary binding sites of hydrogen in a series of metal–organic frameworks composed of  $\text{Zn}_4\text{O}(\text{O}_2\text{C}-)_6$  secondary building units with the use of inelastic neutron scattering from the hindered rotations of the adsorbed molecule. Despite their chemical similarities, the variation in peak positions associated with sites I and II of each MOF is significant and clearly indicates that the organic links play an active role in defining the nature of the adsorption sites for  $\text{H}_2$ . This is reasonable given the variety of links employed in these materials, which strongly affect the local structure of the  $\text{Zn}_4\text{O}(\text{O}_2\text{C}-)_6$  clusters and thus the charge transfer between the  $\text{Zn}^{2+}$  and the aryl carboxylates. In contrast, features assigned to  $\text{H}_2$  bound to primarily organic sites cover a more narrow energy range and show low barriers to rotation consistent with the weaker binding on those sites. These sites show much larger increases in INS intensity with higher  $\text{H}_2$  loading as their capacity for adsorption at the low temperature of these experiments is significantly higher. This conclusion underlines the need to explore new topologies, composed of novel secondary building units from metal cations that have received less attention to increase the binding energies for  $\text{H}_2$  on all sites. In particular, the use of more polarizing centers or the installment of open metal sites should enhance hydrogen physisorption by this class of materials.

**Acknowledgment.** Funding was provided by the NSF, DOE, and BASF. We thank NSERC Canada and the Link Foundation for fellowships to J.L.C.R. We thank Kyo Sung Park for the preparation of 4,5,9,10-tetrahydropyrene-2,7-dicarboxylic acid, Ulrich Müller for providing the IRMOF-8 sample, and Robert Connatser for experimental assistance on the QENS instrument. We would also like to thank Alberto Albinati for helpful discussions. The low-temperature data collections (ref 15) and the insights these provided to this study would not have been possible without the collaboration of Judith A. K. Howard and Elinor C. Spencer (Durham University, UK) and funding of equipment by EPSRC, UK. Work at Los Alamos National Laboratory was supported by the Office of Science, U.S. Department of Energy. The work has benefited from the use of facilities at the Intense Pulsed Neutron Source, a national user facility funded by the Office of Science, U.S. DOE.

**Supporting Information Available:** Complete ref 1e. This material is available free of charge via the Internet at <http://pubs.acs.org>.

JA0542690